DOI: 10.1002/ejic.200500434

Oxo-Entity-Controlled Diastereomer Peculiarity of Rhenium(V) Complexes $ReOX_2(P{\sim}O)py$ [X = Cl, Br, I; P~O = $(OCMe_2CMe_2O)POCMe_2CMe_2O$(1–); py = pyridine]: Synthesis and Molecular and Crystal Structural Characterization

Witold K. Rybak,*[a] Anna Skarżyńska,[a] Ludmiła Szterenberg,[a] Zbigniew Ciunik,[a] and Tadeusz Głowiak[a][†]

Dedicated to Professor Józef J. Ziółkowski on the occasion of his 70th birthday

Keywords: Noncovalent interactions / Crystal engineering / Rhenium complexes / P,O ligand / Density functional calculations

The stability of diastereomers of $ReOX_2(P{\sim}O)py$ complexes determined by the arrangement of the oxo-entity O=Re(–O~P) is manifested in molecular recognition and crystallization behavior [X = Cl, Br, I; P~O = $(OCMe_2CMe_2O)PO$-CMe_2CMe_2O(1–); py = pyridine]. With X = Cl and Br both chiral *cis* [*OC*-6–52] and achiral *trans* [*OC*-6–15] complexes can be obtained concomitantly, while for X = I only a *trans* complex can be afforded. Molecular structures were characterized using NMR IR and UV/Vis spectroscopic methods with the aid of DFT computational analysis and were ultimately corroborated by the single-crystal X-ray diffraction method. These analyses revealed that the most stable diastereomers involve an O=Re(–O~P) oxo arrangement in an axial disposition reinforced with a phosphorus ligating atom mutually *cis* due to extensive π-bonding both for chiral *cis* and achiral *trans* complexes, regardless of whether X = Cl, Br, or I. However, the disparate intramolecular geometry either *cis* or *trans* in the solid state results in enantiomorphic crystals related to space group $P2_12_12_1$ (X = Cl, Br) or crystals pertinent to the centrosymmetric framework $P2_1/c$ (X = Cl, Br, I), respectively. Thoughtful analysis of crystal structures reveals a supramolecular architecture due to intermolecular forces involving hydrogen bonding and electric dipole–dipole interactions (among other contact interactions). Thus, chiral *cis* complexes (X = Cl, Br) show helical crystal packing that succeeds in spontaneous resolution, while *trans* stereoisomers (X = Cl, Br, I) do not and rather exhibit a zig-zag supramolecular framework.

Introduction

The recognition that crystal structure, among other self-assembled systems (e.g. liquid crystals, molecular layers, wires etc.), is the result of a subtle balance between a multitude of supramolecular noncovalent weak forces has attracted much attention to the ability to predict crystal structures.[1] Most efforts are still devoted to searches for a correlation between intramolecular arrangements and crystal packing.[2] The great structural diversity characteristic of transition metal complexes can play a special role in this context both from a theoretical point of view and from the point of view of experimental chemistry applications in crystal engineering and material sciences.[3] The various coordination sites available on the metal center allow ligands to adopt a structural array appropriate to their steric demands and electronic properties. Still, for a given set of metal ligands several stable diastereomeric arrangements are possible showing different molecular properties with consequences for their supramolecular arrangements.[4] Occasionally, a similar potential energy for the diastereomers may result in an isomerization reaction and in the separation of the diastereomers.[5] Several interesting instances of both isomerization and the separation of diastereomers of coordination compounds have been reported recently.[6]

Metal oxo complexes, however, exhibit pronounced anisotropy that might be recognized by other ligands in the molecular stage and by molecules at the supramolecular level.[7] This anisotropy is manifested in multiple bonding within the metal oxo moiety, e.g. the total bond orders are close to three for M=O or near to four for mutually *trans* O=M–OR oxo arrangements. During the course of our studies on the chelating ability of the spirophosphorane ligand HP~O [HP~O = $HP(OCMe_2CMe_2O)_2$][8a,8b]

[a] Faculty of Chemistry, University of Wrocław,
50383 Wrocław, Poland
E-mail: rybak@wchuwr.chem.uni.wroc.pl
[†] Deceased.
Supporting information for this article is available on the WWW under http://www.eurjic.org or from the author.

(Scheme 1) we succeeded in the chirally autocatalytic and highly efficient preparation of one enantiomer (from optically inactive precursors) owing to a subtle interplay between chiral *cis* and achiral *trans* oxo-rhenium complexes $ReOCl_2(P{\sim}O)py$ (py = pyridine).[8c] We reasoned that for a particular set of halide ligands X (X = Cl, Br, I) a specific configuration of the complex should be stabilized. Subsequently, we became interested in the more general question of to what extent one can, by selecting ligands, control the preparation of a certain diastereomer and ultimately its crystal structure including intermolecular recognition and conceivable chiral packing. Breu and co-workers have shown, using the example of trisdiimine-metal chelate complexes, that even a minor intramolecular modification related to metal center ions (Ru or Zn) can drastically alter the packing pattern and crystallization behavior proceeding from racemate to enantiomorph, essentially due to weak intermolecular forces.[9] Known oxo-rhenium complexes of the $ReOX_2(Y{\sim}Z)L$ type, containing an oxo dihalide moiety and a bidentate chelate (Y, Z = O, N, P as ligating atoms) in addition to any other monodentate ligand (L), exhibit either *cis* or *trans* geometry. Chloride complexes mostly adopt the *cis* arrangement,[10] although the *trans* geometry also exists.[11] On the other hand, iodide complexes[12] show a *cis* arrangement, while bromide complexes[13] exhibit *trans* stereochemistry. Thus, no preferential stereochemistry for halide complexes with roughly similar structural frameworks has been observed so far. Obviously, the stereochemistry of those complexes is controlled by much more complex matching of the properties of the ligands and of the metal center. These instances did not allow us to verify our reasoning and consequently gave this work a different focus, especially as we had at our disposal a closely related series of $ReOX_2(P{\sim}O)py$ complexes. In this paper we report on the results of experimental studies, aided computationally by the density functional theory (DFT), on structural characterization of the title diastereomeric complexes, including their syntheses as well as spectroscopic and X-ray single crystal determinations.[14]

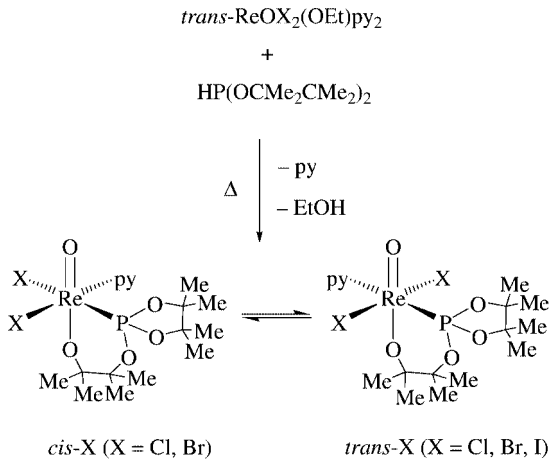

Scheme 1.

Results and Discussion

Synthesis and Spectroscopic Characterization of the $ReOX_2(P{\sim}O)py$ Complexes

The reaction of dihalogeno oxo complexes *trans*-$ReO(OR)X_2py_2$ with an excess of spirophosphorane HP~O, (summarized in Scheme 1) affords corresponding *cis* and/or *trans* $ReOX_2(P{\sim}O)py$ complexes with the new oxo alkoxy entity, O=Re(–O~P), mutually in *trans* disposition. These six-coordinate complexes, besides the monodentate ligands also contain a chelating alkoxy phosphite that derives from a tautomeric deprotonated form of the spirophosphorane $(OCMe_2CMe_2O)POCMe_2CMe_2OH$.[8a,15] Both the chloro and bromo complexes might be isolated in the solid state from the reaction mixture either as the less soluble *cis* or the more soluble *trans* stereoisomer owing to feasible isomerization reactions. Furthermore, certain *cis* or *trans* stereoisomers (X = Cl, Br) can also be obtained from their congeners due to the *cis–trans* equilibration. However, the iodo complex permits only the *trans* isomer. The *cis* and *trans* solubility difference notwithstanding, these complexes are moderately soluble in dichloromethane, acetonitrile, sparingly soluble in toluene, and their solutions are stable at ambient conditions. It is apparent that for the molecular composition of these dihalide $ReOX_2(P{\sim}O)py$ (X = Cl, Br, I) complexes, five chiral *cis* configurations and two achiral *trans* are potentially implicit as depicted in Scheme 2. Configuration indices can been applied to distinguish these diastereomers.[16] Anticipating further discussion of the results, we can for now disclose that *cis*-X-[52] and *trans*-X-[15] are the only synthetically affordable diastereomers.[17]

The relatively distinctive NMR spectra of the obtained complexes are summarized in Table 1. The spectra make it only possible to distinguish between *cis* and *trans* geometry, and no further molecular configuration assignment can be predicted. It is noteworthy that *trans* complexes at room temperature exhibit a C_s ^1H NMR pattern (i.e. four signals related to four enantiotopic pairs of methyl groups) and a long-range coupling $^4J(P,H)$ between ^{31}P and ^1H at the α-position of the py ligand. For *cis* complexes, however, eight resonances related to all the eight methyl groups of the P~O ligand and the absence of a $^{31}P–^1H$ (α-py) coupling corroborate the C_1 symmetry around the metal center and do not reveal much more than this roughly estimated geometry.

IR spectroscopic measurements outlined in the Experimental Section and in the first column of Table 2 are even less distinctive for molecular structure determination. Due to considerable overlapping of the relevant absorption bands, the stretching vibrations attributed to the rhenium-ligating atom set are rather difficult to assign. However, there are exceptions for well-resolved rhenium alkoxo oxygen stretching vibrations ν(Re–O) observed at ca. 621 cm^{-1} both for *cis*-X and *trans*-X complexes. Yet careful examination of the spectral region 1000–900 cm^{-1} by means of mutual comparison of the spectra of all obtained complexes and the spectrum of the free HP~O ligand only makes it possible to tentatively assign the ν(Re=O) vibrations at ca.

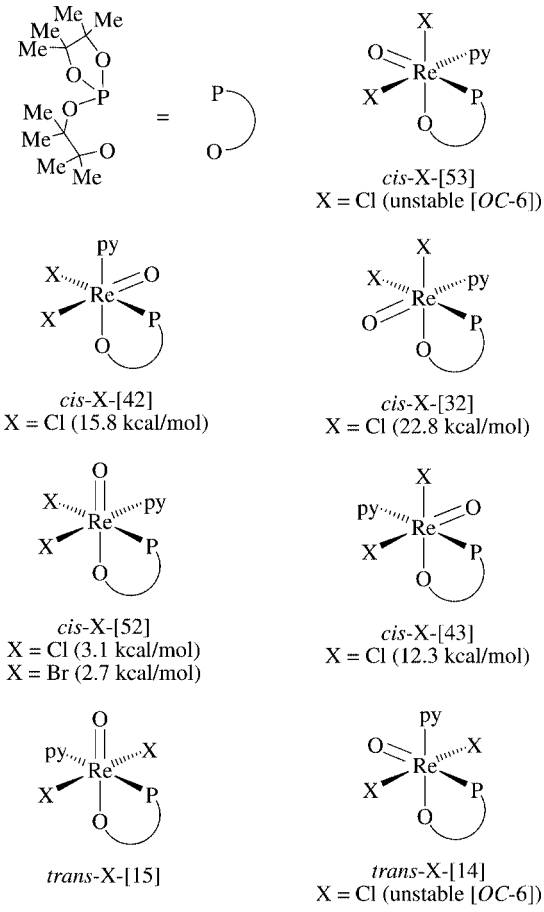

Scheme 2.

956 cm^{-1}, both for *cis* and *trans* complexes. In the low-energy range (FIR), however, ν(Re–X), ν(Re–P), and ν(Re–N) vibrations all occur in a similar region (400–100 cm^{-1}) and straightforward, unambiguous assignment is rather difficult.[18]

Another, fairly indistinctive feature of these complexes is their pink violet color visible in their UV/Vis spectra shown in Table 1. That most likely originates from d–d electronic transitions, which will be discussed later.[19]

To rationalize the above ambiguities in the molecular structure of these complexes and gain insight into their supramolecular arrangements including chirogenesis in the crystal state, more detailed studies were undertaken. The following sections describe molecular electronic structure analyses performed using density functional (DFT) calculations and crystal structure determination supported by single-crystal X-ray analyses.

DFT Computational Analysis of Molecular Structures of $ReOX_2$(P~O)py Diastereomers

This versatile method was used deliberately as it makes it possible to elucidate the experimental uncertainties described above in a reasonable manner and to strike a balance between computational effort and completeness. The primary aim of the computational study was to analyze the relative stability of the seven diastereomers implied above, mainly in the case of the most representative chloride complexes (X = Cl).[20] We expected that general conclusions obtained for the chloride congeners would be largely valid for other halide complexes too. The relative electronic energies for the series *cis*-Cl and *trans*-Cl stereoisomers are shown in Scheme 2. The lowest total electronic energy, and thus the highest stability was found for the *trans*-Cl-[15] configuration located at the bottom left in Scheme 2. Comparison of the calculated relative energy differences reproduces the experimentally observed order of stability of the complexes: achiral *trans*-Cl-[15] > chiral *cis*-Cl-[52] (3.12 kcal mol^{-1}) >> other *cis*- and *trans*-Cl diastereomers (remarkably above 10 kcal mol^{-1}). This low-energy barrier between the Cl-[15] and the Cl-[52] diastereomers supports

Table 1. ^{1}H NMR, ^{31}P NMR, and UV/Vis spectroscopic data of $ReOX_2$(P~O)py complexes.

Complex	^{1}H NMR, δ values [ppm], *J* [Hz]		^{31}P{^{1}H} NMR	UV/Vis
	Methyl	Aryl	δ values [ppm]	λ_{max} [nm] (ε [$M^{-1}cm^{-1}$])
***cis*-Cl**[14]	0.87, 1.31, 1.52, 1.54[a] 1.01, 1.15, 1.40, 1.46[b] (24 H, s)	7.67 (2 H, tm, $^3J_{HH}$ = 7) 7.97 (1 H, tt, $^3J_{HH}$ = 8, $^4J_{HH}$ = 1.6) 8.93 (2 H, dm, $^3J_{HH}$ = 5)	91.03	≈ 650 (30) 499 (147) 314 (4150)
***trans*-Cl**	1.54, 1.57[a] 1.14, 1.41[b] (24 H, s)	7.66 (2 H, tm, $^3J_{HH}$ = 7) 7.98 (1 H, tt, $^3J_{HH}$ = 8, $^4J_{HH}$ = 1.6) 8.83 (2 H, m*, $^4J_{PH}$ ≈ 1)	93.06	≈ 670 (24) 522 (132) 310 (4170)
***cis*-Br**	0.83, 1.27, 1.54, 1.57[a] 1.06, 1.25, 1.44, 1.46[b] (24 H, s)	7.58 (2 H, tm, $^3J_{HH}$ = 7), 7.90 (1 H, tt, $^3J_{HH}$ = 8, $^4J_{HH}$ = 1.6) 8.93 (2 H, dm, $^3J_{HH}$ = 5)	82.73	686 (32) 498 (133) 310 (5720)
***trans*-Br**	1.54, 1.60[a] 1.15, 1.41[b] (24 H, s)	7.67 (2 H, tm, $^3J_{HH}$ = 7), 7.95 (1 H, tt, $^3J_{HH}$ = 8, $^4J_{HH}$ = 1.6), 8.82 (2 H, m*, $^4J_{PH}$ ≈ 1)	95.4	≈ 657 (30) 518 (130) 308 (3850)
***trans*-I**	1.57, 1.62[a] 1.14, 1.40[b] (24 H, s)	7.65 (2 H, tm, $^3J_{HH}$ = 7) 7.96(1 H, tt, $^3J_{HH}$ = 8, $^4J_{HH}$ = 1.6) 8.81(2 H, m*, $^4J_{PH}$ ≈ 1)	103.17	≈ 670 (24) 531 (118) 284 (20800)

[a] Me bound to the five-membered P-containing ring. [b] Me bound to the six-membered rhenium metallacycle ascertained by the 2D NMR experiment. Multiplets consisting of roughly equal intensity signals attributed to the coupling ^{1}H and ^{31}P nucleus based on the 2D NMR experiment are labeled with asterisks *.

Table 2. Important measured and calculated bands in the IR spectra of the $ReOX_2(P{\sim}O)py$ complexes in selected regions.

	Measured bands		Calculated bands	Assignment
***cis*-Cl**	150.1 w		120.6	ν(Re–P)
	239 m	267 vs	213.4	ν(Re–N)
	284.9 s		305.0	ν_{as}(Re–Cl)
	322.6 s		316.9	ν_{s}(Re–Cl)
	869.7 m	927 s	847	ν(C–O) + ν(P–O)
	891 w	942 vs	874	ν(C–O) + ν(P–O)
	956 vs	976 s	956.0	ν(Re=O)
	1014.2 s		1003.0	ν(Re=O) + ν(C–O)
***trans*-Cl**	154.0 w		119.9	ν(Re–P)
	237.4 m	247 s	214.9	ν(Re–N)
			270.5	ν_{s}(Re–Cl)
	302.6 s		293.4	ν_{as}(Re–Cl)
	863.9 m		844	ν(C–O) + ν(P–O)
	895.1 w	931 s	875	ν(C–O) + ν(P–O)
	956 vs	976 s	965.9	ν(Re=O)
	1024 s			
***cis*-Br**	159.7 w		115.7	ν(Re–P)
	180.7 vs	194 s	183	ν_{as}(Re–Br) + ν(Re–N)
	215.6 s		206.3	ν_{s}(Re–Br) + skelet.
	235 m	247 s, 265 s	223.6	ν(Re–N)
	867.7 m	925.7 vs	839.7	ν(C–O) + ν(P–O)
	891.7 w	939.1 vs	873	ν(C–O) + ν(P–O)
	955.9 vs	975 s	956	ν(Re=O)
	1014.6 s		1003.7	ν(Re=O) + ν(C–O)
***trans*-Br**	150.1 vw		127.0	ν(Re–P)
			167.2	ν_{s}(Re–Br) + skelet.
	205.7 vs	179 s		ν_{as}(Re–Br)
	232.5 s	248 m	217.7	ν(Re–N)
	864.5 m	932 vs	843.0	ν(C–O) + ν(P–O)
	895.9 w		875.0	ν(C–O) + ν(P–O)
	956 vs	977.5 s	965.0	ν(Re=O)
	1023.3 s		1013.4	ν(Re–O) + ν(C–O)
***trans*-I**	hidden			ν(Re–P)
			118.0	ν_{s}(Re–I)
	156.4 s		145.5	ν_{as}(Re–I)
	239.9 vs	228 s	226.4	ν(Re–N)
	868.7 m	929 vs	842.9	ν(C–O) + ν(P–O)
	896.9 m	937 vs	874.8	ν(C–O) + ν(P–O)
	957.2 vs	979 m	965.1	ν_{as}(Re=O) + ν(C–O)
	1022.7 m		1012.2	ν_{s}(Re=O) + ν(C–O)

the above-mentioned *cis–trans* isomerization reaction and the feasible separation of *cis* and *trans* complexes.[21] Furthermore, the resulting diastereomer stability trend is in good agreement with the expected promotion and efficiency of the π-donor-acceptor bonding pattern at the metal center with the arrangement of O and P ligating atoms. Phosphorus ligating atoms with their intrinsic π-acidity show a preference to adopt a *cis* disposition with respect to the inherent *trans* O=M–OR oxo arrangement [R = (CMe_2CMe_2O)-$P(OCMe_2CMe_2O)$].[7]

Consequently, the multiply bonded *trans* oxo arrangement is stabilized to some extent due to accessible π-back-donation from rhenium to phosphorus. Other hypothetical diastereomers with mutually *cis* O=M(–OR) oxo arrangements are evidently less encouraging (Scheme 2). Besides, computational studies indicate the lowest stability for pseudo-octahedral complexes [*OC*-6] comprising mutually *cis* oxo arrangements with phosphorus in the *trans* location to the terminal oxygen atom (*trans* -Cl-[14] and *cis* -Cl-[53]), which tend rather to transform to five coordinating species loosing the phosphorus ligand.

Notably, energy differences calculated only for selected bromide and iodide congeners (*trans* -X-[15] and *cis* -X-[52]), assumed to be the most stable, are again in good agreement with the experimental observations. Thus, for bromides, a low energy difference between *trans* -Br-[15] and *cis* -Br-[52] (2.68 kcal mol^{-1}), again implies facile *cis-trans* isomerization. In the case of iodides, *trans* -I-[15] appears to be the only stable complex. To sum up, computational study at this stage dispelled the configuration ambiguity indicating not only the geometry of the most stable diastereomers, X-[15] and X-[52], but also the feasibility of the *cis-trans* isomerization reaction, excluding X = I congeners. For the sake of clarity, below we simply use the abbreviations *trans*-X and *cis*-X for the affordable complexes of X-[15] and X-[52] configurations, respectively.

Afterwards, with computed structures fully optimized using the B3LYP functional, we also tried to deal with am-

biguities in the IR spectra using the DFT method. A summary of the spectral characteristics and stretching vibrations for the *trans*-X and *cis*-X complexes in selected relevant regions are presented in Table 2. Tentative assignment of the observed absorption bands to those calculated was based on the order of their appearance and intensity, in experimental and calculated spectra. In the FIR range, the equivocal position of stretching vibrations ν(Re–P), ν(Re–N), and ν(Re–X) can be verified to some extent. Thus, weak absorption at 150–160 cm^{-1} and medium to strong absorption at 230–240 cm^{-1} can be cautiously assigned to ν(Re–P) and ν(Re–N) vibrations, respectively. Meanwhile, ν(Re–X) absorptions occur in the region of ca. 300 cm^{-1} for ν(Re–Cl), 200 cm^{-1} for ν(Re–Br), and 150 cm^{-1} for ν(Re–I) (accurate values in Table 2), usually as strong bands. Apart from these, ν(Re=O) stretching vibrations resolved using DFT appear, interestingly, at almost invariable positions, 956–957 cm^{-1} for all the attainable complexes. This suggests once more a very stable moiety comprised of ligating phosphorus in *cis* disposition to the oxo arrangement O=M–OR, powered by π-backdonation.

Similarly, the near nonpeculiarity of the electronic absorption spectra intrinsic to complexes with a *cis* or *trans* geometry and the observed complexes with different halides (Table 1) might also suggest that the oxo-metal entity has a controlling nature. With the aim of elucidating this observation in more detail, we performed time-dependent density functional (TDDFT) calculations of the spectral properties. Recently, several computational analyses have been performed for rhenium complexes,[22] which improve the rationalization of their electronic absorption spectra including the related oxo complexes *trans*-$ReO(OEt)Cl_2(L)_2$ (L = py, pyrazine, pyrimidine).[23] Computational analysis has been accomplished in the case of the pair of *trans*-Cl and *cis*-Cl complexes, which represent an exceptional term as a precursor in this series. In comparing the experimental and calculated spectra we consider only the first two bands in the visible range mainly involving the d orbitals. A third, very intensive and higher-energy band occurs in the UV region and is not needed for the purpose of this comparison. The calculated orbital excitations and the corresponding electronic transitions are summarized in Table 3. The assignment of the calculated orbital excitations to the observed absorption bands was guided by an overview of the contour plots and relative energy appropriate to the orbitals HOMO and LUMO involved in the electronic transitions depicted in Figure 1.

The lower-energy excitations are attributed to the two HOMO → LUMO and HOMO → LUMO +1 transitions either for *cis*-Cl or for *trans*-Cl complexes (set 1, Table 3). The contour plots corresponding to these MOs comprise mainly rhenium 5d atomic orbitals (Figure 1). Thus, initial HOMOs involve the rhenium d_{xy} (π*) orbital interacting with chlorine 3p (π*). Both LUMO and LUMO +1 also engage the rhenium d_{xz} (π*) orbital but interact with the π* orbitals of the oxo arrangement. Therefore, the low-energy absorption bands, observed at 650 nm (*cis*-Cl) and 670 nm (*trans*-Cl), can be assigned to d–d (π*) transitions with a certain contribution of metal-to-oxo-ligand charge transfer (MLCT). Two higher-energy excitations, however, are attributed to the two HOMO → LUMO +2 and HOMO → LUMO +4 transitions, which involve rhenium d orbitals but with slightly different contributions (for *cis*-Cl and *trans*-Cl complexes, sets 2–3 in Table 3 and Figure 1). While LUMO +2 comprise substantially pyridine molecular orbitals, easily visible in the contour plots, LUMO +4 again involves mainly rhenium atomic orbitals but with a $d_{x^2-y^2}$ (σ*) symmetry. The observed absorptions at 499 nm (*cis*-Cl) and 522 nm (*trans*-Cl) can be related to a metal-to-pyridine ligand charge transfer (MLCT) with a certain contribution of d (π*)–d (σ*) transitions. Consequently, the similar natures of the above transitions seem to be responsible for the nearly identical absorption spectra at least for *cis* and *trans* chloride complexes.

Table 3. The most important electronic transitions calculated with the TDDFT method: wavelength λ, oscillator strength *f*, and measured λ_{exp} (ε) for *cis*- and *trans*-$ReOCl_2$(P~O)py.

Set	Orbital excitations	λ [nm]	*f*	λ_{exp} [nm] (ε [$M^{-1}\,cm^{-1}$])
***cis*-Cl**				
1	H-(d_{xy} + π* Cl) → L-(d_{yz} + π* O) H-(d_{xy} + π* Cl) → L+1-(d_{xz} + π* O)	717.0	0.001	650 (30)
2	H-(d_{xy} + π* Cl) → L+1-(d_{xz} + π* O) H-(d_{xy} + π* Cl) → L+2-(d_{yz} + π* py)	591.8	0.0007	
3	H-(d_{xy} + π* Cl) → L+2-(d_{yz} + π* py) H-(d_{xy} + π* Cl) → L+4-($d_{x^2-y^2}$ + σ* Cl)	443.3	0.007	499 (147)
***trans*-Cl**				
1	H-(d_{xy} + π* Cl) → L-(d_{xz} + π* O) H-(d_{xy} + π* Cl) → L+2-(d_{xz} + π* py)	678.6	0.004	670 (24)
2	H-(d_{xy} + π* Cl) → L+1-(d_{yz} + π* O)	599.3	0.005	522 (132)
3	H-(d_{xy} + π* Cl) → L+4-($d_{x^2-y^2}$)	421.3	0.0001	

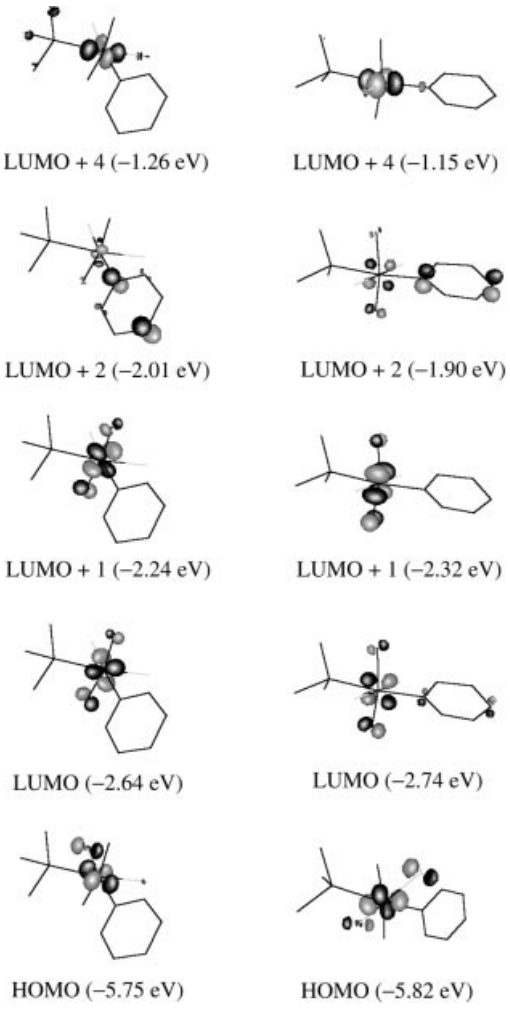

Figure 1. Contour plots relative to selected orbitals HOMO and LUMO active in the electronic transitions in *cis*- (left) and *trans*-$ReOCl_2(P{\sim}O)py$ (right). The orbitals were plotted with the contour values –0.12 (black) and 0.12 au (gray), and referred to the *z*-axis adjacent to the oxygen atoms and the *y*-axis occupied by pyridine and or chlorides. The chlorides are printed in gray.

X-ray Crystal Structure Determination

In general chiral molecules, if they are not pure enantiomers, may form either chiral (conglomerate) or achiral (racemate, racemic solution) crystal structures. Yet, the same might be true for achiral molecules.[24] The question arises what a crystal structure will be if only minor structural changes are applied to a molecule that prior to these changes formed chiral crystals (e.g. Cl^- vs. Br^- ligands or chiral *cis*- vs. achiral *trans*-arrangements) and whether the formation of enantiomorph crystals will still be possible although the molecular structure might now be achiral.

The crystallographic data of $ReOX_2(P{\sim}O)py$ complexes are summarized in Table 5. While two *cis*-X (X = Cl, Br) complexes crystallize in the orthorhombic space group $P2_12_12_1$, as enantiomorphic crystals (conglomerate), three *trans*-X (X = Cl, Br, I) isomers yield monoclinic crystals belonging to the centrosymmetric space group $P2_1/c$. The unit cell of each crystal structure consists of four molecules of $ReOX_2(P{\sim}O)py$ complexes. The packing of the achiral *trans* complexes is slightly less compact (ca. 5% ρ) than that of the chiral *cis* isomers. The Flack parameter, *x*,[25] for selected single chiral crystals of *cis*-Cl [*x* = 0.024(5)] and *cis*-Br [*x* = –0.018(12)] indicates packing with molecules of one enantiomer that accidentally appeared with the opposite absolute configuration of *C* and *A*, respectively. Figure 2 shows the ORTEP drawings with the selected atom numbering schemes for representative *cis*-X (X = Cl) and *trans*-X (X = Cl) complexes. Except for rather insignificant differences related to the coordination of pyridine, the molecular structures do not show extraordinary features in terms of bond lengths and angles. Significant coordination bond lengths and angles for these complexes are submitted in the supporting information in Table S1. All pseudo-octahedral complexes exhibit the characteristic multiply bonded *trans* oxo arrangement, O=Re–O. The rhenium bond lengths with terminal oxo at ca. 1.7 Å and the bridging alkoxo below 1.9 Å are in the usual range, which imply a total bond order of close to four.[7] Furthermore, the coplanarity of the rhenium atom with the plane traced by phosphorus and oxo-moiety donor atoms is a rather meaningful feature of all those complexes. The dihedral angles close to zero between the least-squares planes Re O(1) P and Re O(2) P for *cis*-X [Cl, 4.5(1)°, Br 4.7(2)°] and *trans*-X [Cl, 1.0(1)°, Br 0.0(1)°, I 0.4(2)°], respectively, confirm the approximately coplanar arrangements. This may suggest the remarkable stability of such a four-membered core arrangement, O=Re(–O~P–), due to a versatile π-bonding already anticipated from DFT computational analysis for all the readily affordable diastereomers.

Besides the similarity, there are also some well-pronounced disparities in the intramolecular structures of these stereoisomers between the geometry types, *cis*-X (X = Cl, Br) or *trans*-X (X = Cl, Br, I). Ring puckering analysis[26,27] shows that both fluxional (in solution) five-membered phosphorus and six-membered rhenium cycles in the crystal state adopt conformations relevant for each geometry (i.e. *cis*- or *trans*-), albeit with slight differences between them.[28] Thus, the relevant five-membered phosphorus cycle, -PO4C7C8O5-, embraces the envelope (E) tilted on the enantiotopic carbon atoms, either C7 (*cis*-X) or C8 (*trans*-X). For the relevant six-membered rhenium metallacycles, -RePO2C1C2O3-, tentative inquiries disclose either half-chair (HC) or envelope conformations on C2 for *cis*-X and *trans*-X complexes, respectively.

The molecular peculiarities and similarities discussed above, while subtle, have further consequences in the supramolecular structure and the crystal packing of these stereoisomers. Yet, this might be expected from the molecular self-recognition and self-assembly paradigm[1a,29] for the structure of supramolecular objects and crystals due to weak noncovalent intermolecular forces.[30] These intermolecular interactions might be both directional and nondirectional in nature. To minimize the void volume in 3D structures, molecules tend to pack exploiting weak specific interactions, including directional hydrogen bonds and/or minimal dipole–dipole electrostatic forces. The representative

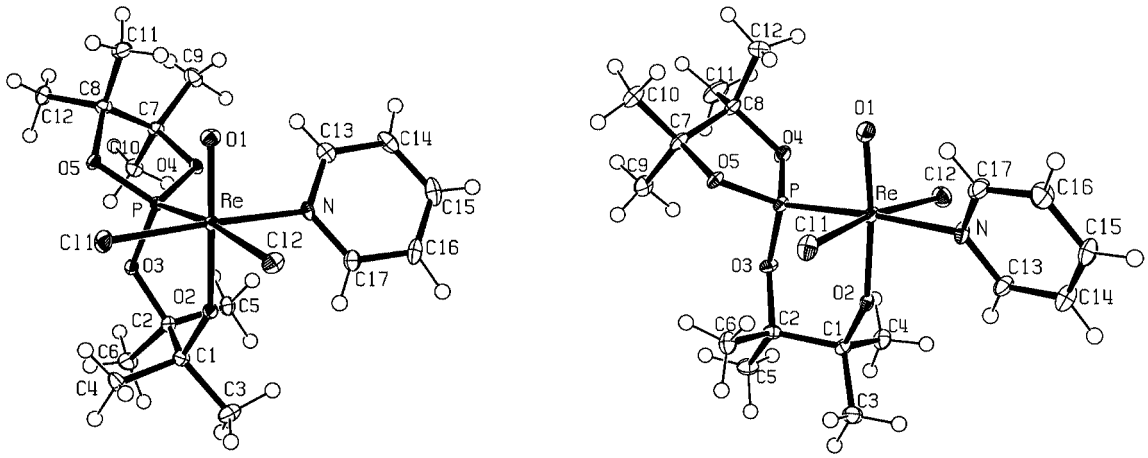

Figure 2. ORTEP molecular diagram (with 30% probability ellipsoids) showing selected atom labeling in *cis*-$ReOCl_2$(P~O)py (left) and *trans*-$ReOCl_2$(P~O)py (right) with hydrogen atoms unlabeled.

modes of crystal packing for *cis*-X (X = Cl) and *trans*-X (X = Cl) complexes are shown in Figures 3 and 4, respectively. Crystals within each stereoisomer type, *cis*-X or *trans*-X (X = Cl, Br), are isomorphous, except for the *trans*-I complex (Table 5). Both *cis*-X and *trans*-X complexes disclose columnar structures in their crystal states. *Cis*-X complexes reveal molecules arranged in cylinders running along the crystallographic axis 2_1, that is parallel to the cell *b* axis (Figure 3), and maintain molecules forming a helical pattern.[31] Meanwhile, *trans*-X complexes exhibit molecules stacked along the *c* axis with stacks mutually related by axis 2_1 parallel to the *b* axis (Figure 4), which sustain them in stacks rather than in any helical structures. The driving noncovalent interactions are obviously responsible for either a cylindrical or stacking disposition of the molecules in the crystals.

Avoiding precarious quantification of the strength of these intermolecular interactions, one can take the opportunity to only roughly classify them. Thoughtful qualitative analysis of the packing shows that molecules might be held together by hydrogen bonds, contact interactions, and dipole–dipole electrostatic interactions.[32] Interactions that are sustained almost twice as often are effected through intermolecular arrangement (11 to 13) rather then by intramolecular arrangement (6 to 7 encounters) for each compound. Notably, in spite of the rather modestly realistic (or very weak) hydrogen bonds involving alkyl hydrogen atoms (H3–H6, H9–H12), the aryl hydrogen atoms (H13–H17) may make an energetically significant contribution to H bonding. This may result in a substantial influence on the type of supramolecular arrangement. With great caution, we can only shed light on the difference in intermolecular

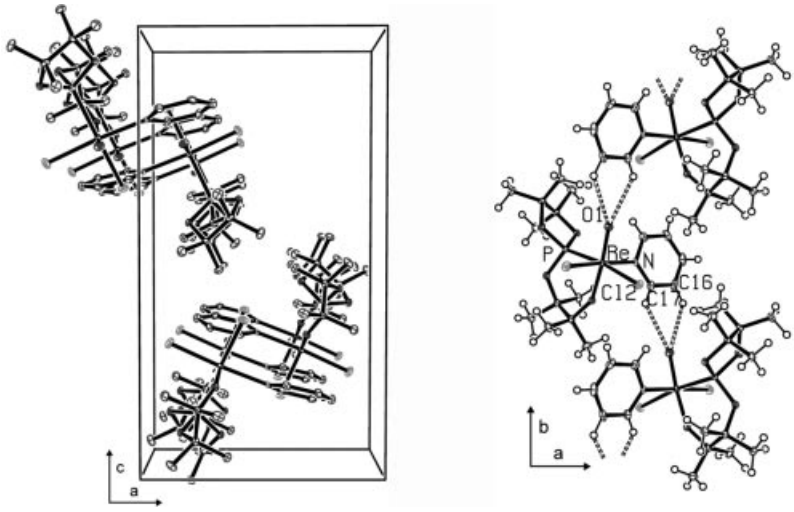

Figure 3. Crystal structure of *cis*-$ReOCl_2$(P~O)py. Perspective view along columns (left), in which molecules are connected by the intracolumn hydrogen bonds (right).

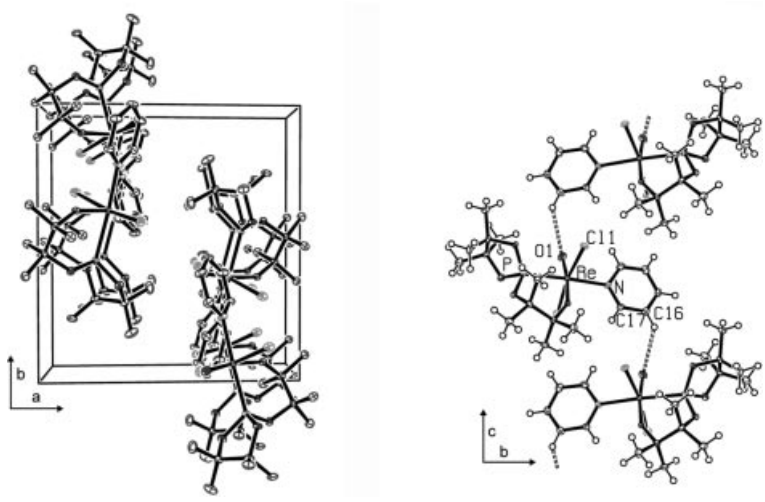

Figure 4. Crystal structure of *trans*-$ReOCl_2(P{\sim}O)py$. Perspective view along columns (left), in which molecules are connected by the intra-column hydrogen bonds (right).

hydrogen bonding acquired by terminal oxygen atoms with both α and β pyridine hydrogen atoms (H17, H16) for *cis*-X (X = Cl, Br, Figure 3, b) and only with β pyridine hydrogen atoms (H16) for *trans*-X (X = Cl, Br, I, Figure 4, b) complexes. Other implied interactions seem to be more concealed and do not allow clear-cut conclusions.[32]

However, on the other hand, the apparent difference in polarity and in the dipole moment[33] between *cis* and *trans* geometry complexes offers an additional possibility of discriminating between intermolecular dipole–dipole electrostatic interactions. In the *cis*-X molecules, a substantial dipole moment (ca. 12.7 D) is pointed out of the most polar bonds and electronegative donor atoms (X1, X2 O1 and O2), whereas in the *trans* stereoisomers a rather moderate dipole moment (ca. 3.15 D) is situated in proximity to the donor atoms, which is depicted in a simplified form in Figure 5. Thus, within each column, the *cis*-X molecules adjust the obtuse angle of the dipole–dipole arrangement, while the *trans* molecules seem not to. We can consider the obtuse angles of dipole arrangements to be a result of the subtle interplay between the tendency towards antiparallel alignment of dipoles and a variety of other weak specific intermolecular forces. This obtuse angle of dipole arrangement (for *cis*-X) allows the bulky part of the molecule to improve accommodation within the column, which manifests itself in a shorter Re–Re distance (e.g. 6.84 Å, X = Cl), as shown in Table 4. In the case of *trans* isomers, substantially smaller dipole moments of molecules are arranged in a parallel way with longer Re–Re distances (e.g. 7.20 Å, X = Cl) within each column. These distances are not too different from inter-column Re–Re distances (e.g. 8.24 Å, X = Cl).

Using this uncomplicated cooperative model, which includes hydrogen bonding and dipole–dipole electrostatic interactions, we can rationalize the supramolecular structure of the title complexes. Both of these specific directional interactions seem to be controlling in the case of *cis*-X complexes. This is manifested in the helical arrangement of the molecules, the shorter Re–Re distance within the column, and the more compact packing. Consequently, this is seen in the greater lattice energies and in the enantiomorphic

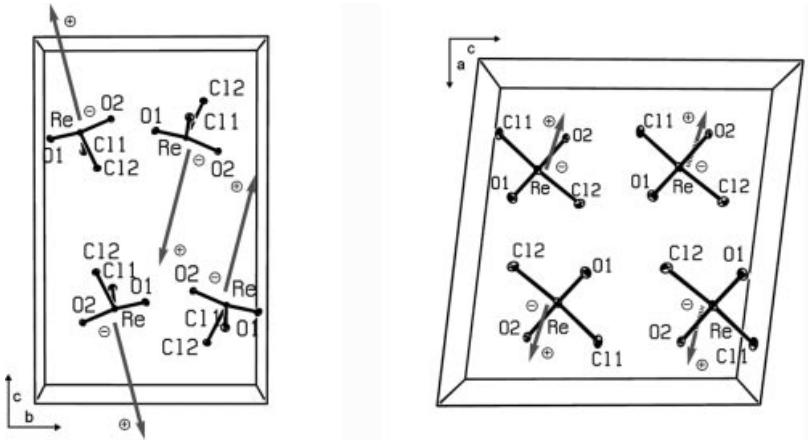

Figure 5. Supramolecular arrangement of molecular dipoles along columns for *cis*-$ReOCl_2(P{\sim}O)py$ (12.65 D, left) and *trans*-$ReOCl_2(P{\sim}O)py$ (3.18 D, right), a schematic overview of the projection of the dipole moments on respective planes.

Table 4. Adjacent intermolecular distances for $ReOX_2$(P~O)py complexes.

Complex	Re–Re distances [Å] Intra-column	Inter-column
cis-Cl	6.84	10.02
trans-Cl	7.20	8.24
cis-Br	6.87	10.20
trans-Br	7.66	8.67
trans-I	8.40	8.25

crystal structures. In contrast, in the case of *trans* geometry complexes, with no dipole–dipole disposition consequences, hydrogen bonding along with other weak interactions including dispersion forces seems to be the operating driving force. This revealed in a stacking arrangement of molecules longer Re–Re distances within the column (Table 4), and less compact packing with a definitely lower lattice energy.

Conclusions

Systematic studies of the title $ReOX_2$(P~O)py complexes definitely illustrate that the oxo entity O=M–OR inherently in *trans* disposition is a building block determining the stability of these diastereomers. Even with this fixed oxo entity, different arrangements of halide ligands are still available, either *trans* or *cis* (X = Cl, Br), implying nonrigidity of these complexes in terms of configuration and conformation. Further, we can stipulate that due to the self-recognition nature of molecules, the molecular structure of the compound may affect the supramolecular arrangement in the crystal state, the eventual spontaneous resolution (X = Cl, Br vs. I), and ultimately chirogenesis. This points to the involvement of fine-tuning in the form of specific interactions involving molecular recognition, which utilize the electronic and steric properties of the ligands and the metal center. We bear in mind the stimulating accounts of Breu and his associates,[9] which showed that for similar complexes with a rigid molecular shape (e.g. $[M(bpy)_3]^{2+}$), a small difference in molecular composition (M = Ni, Zn, Ru) may have a dramatic influence on the form of crystal packing. In fact, that observation validates one of the alternative clear-cut assumptions that crystal structure cannot be predicted.[34] In our case, however, the described structural intramolecular properties and the related intermolecular arrangements of the molecules do not seem to corroborate the above assumption. Replacements of halides do not dramatically alter the packing pattern. Both chloride and bromide complexes can crystallize in the orthorhombic ($P2_12_12_1$) and monoclinic centrosymmetric ($P2_1/c$) space groups, depending intimately on their intramolecular geometry. Consequently, these observations seem to support the alternative statement of Grepioni, Braga, and co-workers that "objects of similar shape tend to pack in a similar manner."[35] It is noteworthy that in our system, the related molecules exhibit pronounced anisotropy owing to the oxo arrangement and are not rigid. This obviously convenient case makes it possible to utilize intramolecular degrees of freedom and optimize the similar packing for the corresponding halide (X = Cl, Br, I) diastereomers.

Experimental Section

All preparations were performed under dry, oxygen-free nitrogen, using conventional Schlenk techniques. Solvents were carefully dried and deoxygenated by standard methods.[36] *trans*-$ReOX_2$(OEt)py_2 (X = Cl, Br, I),[37] *cis*-$ReOCl_2$(P~O)py[8a], and the ligand $HP(OCMe_2CMe_2O)_2$[8a] were prepared according to literature procedures.

IR and FIR measurements were performed in KBr pellets either with a Nicolet FTIR Impact 400 or in Nujol with a Bruker IFS 113V. ^1H, ^{13}C, ^{31}P NMR spectra were obtained with a Bruker AMX (300 MHz for ^1H NMR). The chemical shifts (δ) are given in ppm towards the TMS (^1H, ^{13}C) and H_3PO_4 (^{31}P) using deuterated solvents as lock and reference (^1H, ^{13}C), respectively. 2D NMR and ^1H-^{31}P COSY experiments made it possible to distinguish and unambiguously assign the chemical shifts of methyl groups attributed to both phosphorocycles and metallacycles (Table 1). UV/Vis spectra in CH_2Cl_2 solution were obtained with a Carry 500. Elemental analyses were performed with a Perkin–Elmer 2400 CHN by the Laboratory of Elemental Analyses in our Department.

***trans*-$ReOCl_2$(P~O)py (*trans*-Cl):** Finely ground crystalline *cis*-[$ReOCl_2${$OCMe_2CMe_2OP(OCMe_2CMe_2O)$}py] (0.025 g, 0.04 mmol) was added to toluene (50 mL). It was vigorously stirred and slowly distilled (over 1 h) to about 25 mL. After cooling to room temperature, the remaining solid, which appeared to be the starting *cis* complex, was filtered (0.0024 g, 9.6%). The mother liquor yielded crystals (0.018 g, 72%) of pure *trans*-[$ReOCl_2${$OCMe_2CMe_2OP(OCMe_2CMe_2O)$}py]. Single crystals suitable for X-ray analysis were obtained by re-crystallization from a dichloromethane/ethyl ether solution as a purple-violet compound. $C_{17}H_{29}Cl_2NO_5PRe$ (615.5): calcd. C 33.17, H 4.75, N 2.28; found C 33.5, H 4.65, N 2.52. IR (KBr): $\tilde{\nu}$ = 623.0 [m, ν(Re–O)], 931.8 (s), 956.3 [vs., ν(Re=O)], 1024.7 [s, ν(C–O–P)], 1608.4 [m, ν(C=N)] cm^{-1}; FIR (nujol): 154.0 (w), 237.4 (m), 247(s), 302.6 [ν(Re–P)], ν(Re–N), ν(Re–Cl) cm^{-1}. The compound was also isolated as a side product from the toluene filtrate remaining after the preparation of the isomer *cis*. The filtrate was evaporated to dryness, the residue washed several times with pentane and ethyl ether, than crystallized from toluene with ca. 8% yield. In addition, when the sample of the pure *trans*-Cl complex (0.066 g) was placed in boiling toluene (10 mL) for 1 h, it again afforded the *cis*-Cl complex (65%) as a solid, which proves the isomerization reaction.

***cis*-$ReOBr_2$(P~O)py (*cis*-Br):** A suspension of the blue complex $ReOBr_2$(OEt)py_2 (0.395 g, 0.699 mmol) and the spirophosphorane ligand $HP(OCMe_2CMe_2O)_2$ (0.341 g, 1.292 mmol) in toluene (25 mL) was stirred and boiled for 6 h until the starting rhenium compound reacted and a light-violet crystalline solid was afforded. The product was filtered, washed with Et_2O, and dried in vacuo (0.368 g, 74.8%). Single crystals suitable for X-ray analysis were obtained by crystallization from a dichloromethane/ethyl ether solution as a purple-violet compound. $C_{17}H_{29}Br_2NO_5PRe$ (704,4): calcd. C 28.99, H 4.15, N 1.99; found C 29.06, H 3.93, N 2.07. IR (KBr): $\tilde{\nu}$ = 618.6 [m, ν(Re–O)], 925.7 (vs), 955.9 [vs., ν(Re=O)], 1014.6 [s, ν(C–O–P)], 1605.3 [m, ν(C=N)] cm^{-1}; FIR (nujol) 159.7 (w), 180.7(s), 215.6(s), 235[m, ν(Re–Br)], ν(Re–N), ν(Re–P) cm^{-1}.

***trans*-$ReOBr_2$(P~O)py (*trans*-Br):** A suspension of the pink-violet compound *cis*-$ReOBr_2$(P~O)py (0,05 g, 0,071 mmol) in toluene

(50 mL) was stirred and boiled for 1 h. After cooling to room temperature, the remaining *cis*-$ReOBr_2(P{\sim}O)py$ solid was filtered. The remaining solution was evaporated to dryness affording *trans*-$ReOBr_2(P{\sim}O)py$ (0.04 g, 80%). Single crystals suitable for X-ray analysis were obtained by crystallization from a dichloromethane/ethyl ether solution as a purple-violet compound. Besides, this complex was afforded as a side product from the remaining toluene filtrate obtained in the *cis*-Br preparation, by a method similar to that used for *trans*-Cl, with ca. 12% yield. $C_{17}H_{29}Br_2NO_5PRe$ (704.4): calcd. C 28.99, H 4.15, N 1.99; found C 29.0, H 4.09, N 2.02. IR (KBr): $\tilde{\nu}$ = 622.9 [m, ν(Re–O)], 931.9 (vs), 955.9 [vs., ν(Re=O)], 1023.3 [s, ν(C–O–P)], 1609.1 [m, ν(C=N)] cm^{-1}; FIR (nujol) 150.1 (vw), 179 (s), 205.7 (vs), 232 (s), 248 [m, ν(Re–P)], ν(Re–Br), ν(Re–N) cm^{-1}.

***trans*-$ReOI_2(P{\sim}O)py$ (*trans*-I):** A mixture of $ReOI_2(OEt)py_2$ (0.359 g, 0.545 mmol), toluene (25 mL), and the spirophosphorane ligand $HP(OCMe_2CMe_2O)_2$ (0.279 g, 1.059 mmol) was stirred and boiled for 6 h until the starting rhenium compound reacted and new a deep-orange solution appeared. The solution was concentrated in vacuo by half to obtain a red-violet precipitate of $ReOI_2(P{\sim}O)py$. The product was filtered, washed with Et_2O and dried (0.38 g, 87%). Single crystals suitable for X-ray analysis were obtained by crystallization from dichloromethane/ethyl ether solution as a red-violet compound. For $C_{17}H_{29}I_2NO_5PRe$ (798,41): calcd. C 25.57, H 3.66, N 1.75; found C 25.66, H 3.34, N 2.00. IR (KBr): $\tilde{\nu}$ = 622.6 [m, ν(Re–O)], 929.5 (vs), 957.2 [vs., ν(Re=O)], 1022.7 [m, ν(C–O–P)], 1606.6 [m, ν(C=N)] cm^{-1}; FIR (nujol) 156.4 (s), 228 (s), 239.9 (vs), ν(Re–P), ν(Re–I), ν(Re–N) cm^{-1}.

Computational Analysis: The calculations were carried out with the GAUSSIAN 2003 program.[38] All structures were optimized starting from experimental geometries (X-ray) with no symmetry restrictions, using the Kohn–Sham density functional theory (DFT) with Becke's three-parameter[39] exchange functionals and the gradient-corrected functionals of Lee, Yang, and Parr [DFT(B3LYP)] with the SDD basis set. Vibrational frequencies were calculated in order to confirm the nature of the stationary points and to achieve the zero-point energies (ZPEs). Calculations of electronic spectra were performed at the TDDFT level. Molecular structures were visualized using the program MOLDEN.[40] Molecular orbitals were drawn by the program gOpenMol.[41] The programs ORTEP[42] and GSVIEW[43] were used for graphical presentation of crystallographic results. Cartesian coordinates for optimized structures have been deposited with the Supporting Information.

Crystal Structure Determination: Crystal data for *cis*- and *trans*-$ReOX_2(P{\sim}O)py$ complexes are summarized in Table 5. The data collected with the KM4CCD diffractometer were corrected for Lorentz and polarization effects. Data reduction and analysis were carried out using the Oxford Diffraction (Poland) programs. The structure was solved by means of heavy atom methods using SHELXS-97 and refined by the full-matrix least-squares method on F^2 using SHELXL-97 procedures (G. M. Sheldrick, University of Göttingen, Germany, **1997**). Non-hydrogen atoms were refined with anisotropic thermal parameters. Hydrogen atoms were included from the Δρ maps and refined with isotropic thermal parameters. Crystallographic data (excluding structure factors) for the structures reported in this paper have been deposited with the Cambridge Crystallographic Data Center (CCDC) as a supplementary publication. CCDC-167174 (for *cis*-Cl) and -271243 ... -271246 contain the supplementary crystallographic data for this paper. These data can be obtained free of charge from The Cambridge Crystallographic Data Centre via www.ccdc.cam.ac.uk/data_request/cif.

Supporting Information (details see footnote on the first page of this article): A PDF file with supporting information for this article is also available from the authors. It contains tables showing the relevant bond lengths and angles (Table S1), the ring puckering analysis (Table S2), the analysis of possible hydrogen bonding and contacts (Table S3), and color versions of Figures 1, 3, and 4, which ensure better visualization of the 3D structures (Figure S1, S2, and S3, respectively).

Table 5. Crystallographic data for *cis*- and *trans*-$ReOX_2(P{\sim}O)py$ complexes.

	cis-Cl[8c]	*trans*-Cl	*cis*-Br	*trans*-Br	*trans*-I
Empirical formula	$C_{17}H_{29}Cl_2NO_5PRe$	$C_{17}H_{29}Cl_2NO_5PRe$	$C_{17}H_{29}Br_2NO_5PRe$	$C_{17}H_{29}Br_2NO_5PRe$	$C_{17}H_{29}I_2NO_5PRe$
Formula weight	615.48	615.48	704.39	704.39	798.38
Temperature [K]	100(1)	100(2)	293(2)	100(1)	100(2)
Color	pink violet	pink violet	pink violet	pink violet	red violet
Crystal size [mm]	0.15×0.10×0.10	0.15×0.14×0.12	0.20×0.17×0.14	0.15×0.10×0.06	0.23×0.17×0.14
Space group	$P2_12_12_1$ (No.19)	$P2_1/c$ (No.14)	$P2_12_12_1$	$P2_1/c$	$P2_1/c$
a [Å]	9.988(2)	13.2196(12)	10.124(2)	12.579(2)	16.0501(8)
b [Å]	11.655(2)	13.8204(12)	11.756(2)	13.870(1)	10.0633(5)
c [Å]	18.301(4)	12.3231(12)	18.632(4)	13.338(2)	16.8049(11)
α [°]	90.00	90.00	90.00	90.00	90.00
β [°]	90.00	97.077(8)	90.00	95.05(3)	118.313(6)
γ [°]	90.00	90.00	90.00	90.00	90.00
V [Å^3]	2130.4(7)	2234.3(4)	2217.5(7)	2316.50(16)	2389.6(2)
Z	4	4	4	4	4
$\rho_{calcd.}$ ($Mg\,m^{-3}$)	1.919	1.830	2.110	2.020	2.219
λ [Å]	0.71073	0.71073	0.71073	0.71073	0.71073
μ [mm^{-1}]	6.057	5.776	9.182	8.784	7.761
F(000)	1208	1208	1352	1352	1496
θ range [°]	3.49 ≤ 28.64	3.33 ≤ 27.00	3.44 ≤ 27.00	3.07 ≤ 27.00	3.16 ≤ 27.99
Reflections collected	14435	14659	14696	17528	28809
Unique reflections	5031	4809	4819	4971	5750
R_1/wR_2 indices[f]	0.0195/0.0514[a]	0.0311/0.0724[b]	0.0371/0.0700[c]	0.0288/0.0596[d]	0.0226/0.0388[e]

[a] a = 0.0308, b = 0.9807. [b] a = 0.0418, b = 0.0. [c] a = 0.0181, b = 0.0. [d] a = 0.0274, b = 0.0. [e] a = 0.0172, b = 0.0. [f] Calcd. $w = 1/[\sigma 2(F_o^2) + (aP)^2 + bP]$, where $P = (F_o^2 + F_c^2)/3$.

Acknowledgments

The quantum calculations were carried out at the Poznań Supercomputer Center (Poznań) and Wrocław Supercomputer Center (Wrocław).

[1] a) J. M. Lehn, J. L. Atwood, J. E. D. Davies, D. D. MacNicol, F. Vögtle (Eds.), *Comprehensive Supramolecular Chemistry*, Pergamon, Oxford, **1996**; b) D. Braga, F. Grepioni, *Chem. Commun.* **1996**, 571–578; c) C. B. Aakeröy, *Acta Crystallogr., Sect. B* **1997**, *53*, 569–586.

[2] a) J. A. R. P. Sarma, G. R. Desiraju, *Cryst. Growth Des.* **2002**, *2*, 93–100; b) P. Verwer and F. J. J. Leusen in *Reviews in Computational Chemistry* (Eds.: K. B. Lipkowitz, D. B. Boyd), Wiley-VCH, New York, **1998**, vol. 12, pp. 327–365; c) W. D. S. Motherwell, H. L. Ammon, J. D. Dunitz, A. Dzyabchenko, P. Erk, A. Gavezzotti, D. W. M. Hofmann, F. J. J. Leusen, J. P. M. Lommerse, W. T. M. Mooij, S. L. Price, H. Scheraga, B. Schweizer, M. U. Schmidt, B. P. van Eijck, P. Verwer, D. E. Williams, *Acta Crystallogr., Sect. B* **2002**, *58*, 647–661; d) S. M. Woodley, P. D. Battle, J. D. Gale, C. R. A. Catlow, *Phys. Chem. Chem. Phys.* **2004**, *6*, 1815–1822; e) S. M. Woodley, *Structure Bonding* **2004**, *110*, 95–132.

[3] a) D. Braga, F. Grepioni, *Acc. Chem. Res.* **2000**, *33*, 601–608; b) J. Breu, H. Domel, P. O. Norrby, *Eur. J. Inorg. Chem.* **2000**, 2409–2419; c) V. V. Borovkov, T. Harada, Y. Inoue, R. Kuroda, *Angew. Chem. Int. Ed.* **2002**, *41*, 1378–1381; d) C. Janiak, *Dalton Trans.* **2003**, *14*, 2781–2804; e) S. L. James, *Chem. Soc. Rev.* **2003**, *32*, 276–288; f) G. R. Desiraju, *J. Mol. Struct.* **2003**, *656*, 5–15; g) L. Brammer, *Chem. Soc. Rev.* **2004**, *33*, 476–489; h) D. Huttner, J. Breu, *Z. Anorg. Allg. Chem.* **2004**, *630*, 2527–2531.

[4] A. von Zelewsky, *Stereochemistry of Coordination Compounds*, Wiley, New York, **1996**.

[5] R. G. Wilkins, *Kinetics and Mechanism of Reactions of Transition Metal Complexes*, 2nd ed., VCH, Weinheim, **1991**.

[6] a) Y. Ihara, R. Nakamura, *Thermochim. Acta* **1997**, *302*, 211–214; b) E. H. S. Sousa, C. P. Oliveira, L. C. G. Vasconcellos, L. G. F. Lopez, I. C. N. Diógenes, I. M. M. Carvalho, J. C. V. Miranda, F. A. Dias, I. S. Moreira, *Thermochim. Acta* **2001**, *376*, 141–145; c) Y. Takashima, Y. Nakayama, H. Yasuda, A. Nakamura, A. Harada, *J. Organomet. Chem.* **2002**, *664*, 234–244; d) M. S. Hannu-Kuure, J. Komulainen, R. Oilunkaniemi, R. S. Laitinen, R. Suontamo, M. Ahlgren, *J. Organomet. Chem.* **2003**, *666*, 111–120; e) F. M. Nareetsile, O. P. M. Horwood, D. G. Billing, D. C. Levendis, N. J. Coville, *J. Organomet. Chem.* **2003**, *682*, 2–7.

[7] a) C. J. L. Lock, G. Turner, *Can. J. Chem.* **1977**, *55*, 333–339; b) C. J. L. Lock, G. Turner, *Can. J. Chem.* **1978**, *56*, 179–188; c) J. M. Mayer, *Inorg. Chem.* **1988**, *27*, 3899–3903; d) W. A. Nugent, *Metal Ligand Multiple Bonds*, Wiley, New York, **1988**; e) T. S. Franczyk, K. R. Czerwinski, K. N. Raymond, *J. Am. Chem. Soc.* **1992**, *114*, 8138–8146.

[8] a) T. Głowiak, W. K. Rybak, A. Skarżyńska, *Polyhedron* **2000**, *19*, 2667–2672; b) A. Skarżyńska, W. K. Rybak, T. Głowiak, *Polyhedron* **2001**, *20*, 2667–2674; c) W. K. Rybak, A. Skarżyńska, T. Głowiak, *Angew. Chem. Int. Ed.* **2003**, *42*, 1725–1727.

[9] a) J. Breu, H. Domel, A. Stoll, *Eur. J. Inorg. Chem.* **2000**, 2401–2408; b) J. Breu, W. Seidl, D. Huttner, F. Kraus, *Chem. Eur. J.* **2002**, *8*, 4454–4460.

[10] a) M. B. Hursthouse, S. A. A. Jayaweera, A. Quick, *J. Chem. Soc., Dalton Trans.* **1979**, 279–282; b) T. I. A. Gerber, J. Bruwer, G. Bandoli, J. Perils, J. G. H. du Preez, *J. Chem. Soc., Dalton Trans.* **1995**, 2189–2192; c) F. Tisato, F. Refosco, C. Bolzati, A. Cagnolini, S. Gatto, G. Bandoli, *J. Chem. Soc., Dalton Trans.* **1997**, 1421–1427; d) T. I. A. Gerber, J. Perils, J. G. H. du Preez, G. Bandoli, *Acta Crystallogr., Sect. C* **1997**, *53*, 217–219; e) Xiaoyuan Chen, F. J. Femia, J. W. Babich, J. Zubieta, *Inorg. Chim. Acta* **2000**, *306*, 113–116; f) Xiaoyuan Chen, F. J. Femia, J. W. Babich, J. Zubieta, *Inorg. Chim. Acta* **2000**, *308*, 80–90.

[11] G. Bandoli, S. Gatto, T. I. A. Gerber, J. Perils, J. G. H. du Preez, *J. Coord. Chem.* **1996**, *39*, 299–312.

[12] S. M. O. Quintal, H. I. S. Nogueira, V. Felix, M. G. B. Drew, *New J. Chem.* **2000**, *24*, 511–517.

[13] V. Bertolasi, M. Sacerdoti, G. Gilli, U. Mazzi, *Acta Crystallogr. Sect. B* **1982**, *38*, 426–429.

[14] Although some chemical properties of $ReOCl_2$(P~O)py have been reported previously (see ref.[8a,c]), this work comprises either updated (NMR UV/Vis) or new results. Furthermore, their detailed molecular and crystal structure has not been discussed before.

[15] a) D. Bernard, C. Laurenco, R. Burgada, *J. Organomet. Chem.* **1973**, *47*, 113–123; b) R. Burgada, *Bull. Soc. Chim. Fr.* **1975**, 407–424.

[16] IUPAC, *Nomenclature of Inorganic Chemistry. Recommendations* (Ed.: G. J. Leigh), Blackwell, Oxford, **1992**.

[17] For the sake of brevity we adopt the abbreviated form of configuration indices, for example [52] instead of the long form [*OC*-6-52].

[18] K. Nakamoto, *Infrared Spectra of Inorganic and Coordination Compounds*, 4th ed., Wiley Interscience, New York, **1986**.

[19] a) A. B. P. Lever, *Inorganic Electronic Spectroscopy*, 2nd ed., Elsevier, Toronto, **1984**; b) M. Baluka, J. Hanuza, B. Jezowska-Trzebiatowska, *Bull. Acad. Pol. Sci. Ser. Sci. Chim.* **1972**, *20*, 271–278.

[20] These chloride complexes, and in particular *trans*-Cl and *cis*-Cl appear to be the most effective in terms of enantioselectivity in chirally autocatalytic syntheses; see ref.[8c].

[21] Other details on *cis–trans* equilibration contained in the paper dealing with the mechanism of chiral amplification will be reported elsewhere.

[22] a) J. Bossert, N. B. Amor, A. Strich, C. Daniel, *Chem. Phys. Lett.* **2001**, *342*, 617–624; b) B. Machura, M. Jaworska, R. Kruszynski, *Polyhedron* **2004**, *23*, 1819–1827; c) B. Machura, *Polyhedron* **2004**, *23*, 2363–2371.

[23] a) E. Iengo, E. Zangrando, S. Mestroni, G. Fronzoni, M. Stener, E. Alessio, *J. Chem. Soc., Dalton Trans.* **2001**, 1338–1346.

[24] J. Jacques, A. Collet, S. H. Wilen, *Enantiomers, Racemates and Resolutions*, W. Krieger Publishing, Malabar, FL, USA, **1994**.

[25] a) H. D. Flack, *Acta Crystallogr., Sect. A* **1983**, *39*, 876–881; b) H. D. Flack, G. Bernardinelli, *J. Appl. Crystallogr.* **2000**, *33*, 1143–1148; c) H. D. Flack, *Helv. Chim. Acta* **2003**, *86*, 905–921.

[26] a) D. Cremer, J. A. Pople, *J. Am. Chem. Soc.* **1975**, *97*, 1354–1358; b) D. Cremer, *Acta Crystallogr., Sect. B* **1984**, *40*, 498–500; c) S. T. Rao, E. Westhof, M. Sundaralingam, *Acta Crystallogr. Sect. A* **1981**, *37*, 421–425.

[27] A. L. Spek, *J. Appl. Crystallogr.* **2003**, *36*, 7–13 [A. L. Spek, *PLATON, A Multipurpose Crystallographic Tool*, Utrecht University, The Netherlands, **2002** (http://www.cryst.chem.uu.nl/platon.)].

[28] Electronic Supporting Information: C&P and Sundaralingam ring puckering analysis and its parameters are presented in Table S2.

[29] a) J. M. Lehn, *Pure Appl. Chem.* **1994**, *66*, 1961–1966; b) J. D. Dunitz, *Acta Crystallogr., Sect. B* **1995**, *51*, 619–631; c) L. Perez-Garcia, D. B. Amabilino, *Chem. Soc. Rev.* **2002**, *31*, 342–356.

[30] a) A. I. Kitaigorodskii, *Molecular Crystal and Molecules*, Academic Press, New York, **1973**; b) G. R. Desiraju (Ed.), *Perspectives in Supramolecular Chemistry*, Wiley, Chichester, **1966**, vol. 2.; c) G. R. Desiraju, T. Steiner, *The Weak Hydrogen Bond in Structural Chemistry and Biology*, Oxford University Press, Oxford, **1999**.

[31] The 2_1 screw axis operates either in a clockwise or anti clockwise manner with the same result. Yet, the path of a helix can be traced if intermolecular hydrogen bonds, O1···Hpy, between adjacent molecules in the columns are distinguished (Figure 3).

[32] Electronic Supporting Information: The geometry of the possible inter- and intramolecular hydrogen bonds, and contact interactions is presented in Table S3.
[33] Total dipole moments, its orientations were calculated with GAUSSIAN for isolated molecules and yielded: *cis*-X-[52] 12.65 D (X = Cl), 12.76 D (X = Br), *trans*-X-[15] 3.18 D (X = Cl), 3.08 D (X = Br), 3.22 D (X = I), respectively.
[34] A. Gavezzotti, *Acc. Chem. Res.* **1994**, *27*, 309–314.
[35] F. Grepioni, G. Cojazzi, S. M. Drapper, N. Scully, D. Bragga, *Organometallics* **1998**, *17*, 296–307.
[36] D. D. Perrin, W. L. F. Armarego, *Purification of Laboratory Chemicals*, 3rd ed., Pergamon Press, Oxford, **1988**.
[37] M. Freni, D. Giusto, P. Romiti, G. Minghetti, *Gazz. Chim. Ital.* **1969**, *99*, 286–299.
[38] M. J. Frisch, G. W. Trucks, H. B. Schlegel, G. E. Scuseria, M. A. Robb, J. R. Cheeseman, J. A. Montgomery, Jr. T. Vreven, K. N. Kudin, J. C. Burant, J. M. Millam, S. S. Iyengar, J. Tomasi, V. Barone, B. Mennuci, M. Cosssi, G. Scalmani, N. Rega, G. A. Petersson, H. Nakatsuji, M. Hada, M. Ehara, K. Toyota, R. Fukuda, J. Hasegawa, M. Ishida, T. Nakajima, Y. Honda, O. Kitao, H. Nakai, M. Klene, X. Li, J. E. Knox, H. P. Hratchian, J. B. Cross, C. Adamo, J. Jaramilo, R. Gomperts, R. E. Stratmann, O. Yazyew, A. J. Austin, R. Cammi, C. Pomelli, J. W. Ochterski, P. Y. Ayal, K. Morokuma, G. A. Voth, P. Salvador, J. J. Dannenberg, V. G. Zakrzewski, S. Dapprich, A. D. Daniels, M. C. Strain, O. Farkas, D. K. Malick, A. D. Rabuck, K. Raghavachari, J. B. Foresman, J. V. Ortiz, Q. Cui, A. G. Baboul, S. Clifford, J. Cioslowski, B. B. Stefanov, G. Liu, A. Liashenko, P. Piskorz, I. Komaromi, R. L. Martin, D. J. Fox, T. Keith, M. A. Al.-Laham, C. Y. Peng, A. Nanayakkara, M. Challacombe, P. M. W. Gill, B. Johnson, W. Chen, M. W. Wong, C. Gonzalez, J. A. Pople, Gaussian, Inc., Pittsburgh, PA, **2003**.
[39] a) A. D. Becke, *Phys. Rev. A* **1988**, *38*, 3098–3100; b) C. Lee, W. Yang, R. G. Parr, *Phys. Rev. B* **1988**, *37*, 785–789; c) B. G. Johnson, P. M. W. Gill, J. A. Pople, *J. Chem. Phys.* **1993**, *98*, 5612–5626; d) A. D. Becke, *J. Chem. Phys.* **1993**, *98*, 5648–5652.
[40] G. Schaftenaar, *Molden*, Release 3.6, CMBI, The Netherlands, **2000**, http://www.caos.kun.nl/schft/molden/molden.html.
[41] L. Laaksonen, *gOpenMol* program for the display and analysis of molecular structures, version 2.00, Center for Scientific Computing, Espoo, Finland, **1997**–**2001**, http://www.csc.fi/gopenmol/index.phthml.
[42] a) L. J. Farrugia, *J. Appl. Crystallogr.* **1999**, *32*, 837–838; b) Program based on *ORTEP III* by C. K. Johnson and N. N. Burnett; L. J. Farrugia, University of Glasgow, **1997**–**2005**.
[43] R. Lang, *GSVIEW 32*, Ghostgum Software Pty Ltd., **2003**, http://www.ghostgum.com.au/.

Received: May 12, 2005
Published Online: November 2, 2005

